Fermilab

MONTE CARLO STUDIES ON TEVATRON EXTRACTION

M. Harrison

October 26, 1979

In this report we present some initial results obtained from a Monte Carlo simulation of fast resonant extraction. We have looked at the behavior of extraction in the presence of the skew harmonics in the dipole magnets with and without skew correcting elements; the effect of chromaticity and off-momentum orbits, and the consequences of randomly distributing the lower order normal dipole harmonics as well as the skew fields.

The program was set up to simulate a fast extraction cycle with the extraction devices as given in Table 8.1 of the Design Report (slow quadrupoles and octopoles at stations 28-42 together with fast quadrupoles at the 48 locations). The slow extraction devices are set to constant values throughout the extraction cycle bringing the beam close to the one-half integer resonance and providing the necessary non-linearities to define the stable and unstable phase space regions. The beam is then brought into resonance by applying a 3.0 msec half sine wave pulse to the fast quadrupoles. The magnitude of this pulse is then adjusted to give a 1.0 msec extracted beam spill. Figure 1 shows the time dependence of the pulsed waveform together with the extracted beam spill for a typical extraction cycle. Figure 2 is a photograph of the same waveforms taken during the standard operation of the Main Ring. The

(barely visible) time scale of the oscilloscope trace is 1 msec/div. The agreement between figures 1 and 2 is reasonably good.

The basic mechanics of the program are relatively straightforward. Each particle is projected through each lattice element sequentially, the higher order dipole fields are used to generate angular displacements which are added to the particle trajectories at the center of each dipole. No higher order terms are included for the lattice quadrupoles as these are insignificant compared to the dipole terms. The initial particle distributions, generated in random gaussian form at the center of the F0 long straight section, are shown in Fig. 3 which gives the initial horizontal (or vertical) phase space together with both projections and the momentum distribution. These initial conditions correspond to a transverse phase space emittance of 0.1π mm-mrad (99%) together with a momentum spread of $\Delta p/p \leq \pm 0.025\%$ (99%). Unless explicitly stated these distributions are used throughout this report as the initial conditions. Figures 4 and 5 show the horizontal phase space evolution during the cycle at the upstream end of the electrostatic and magnetic septa respectively. Throughout this report we shall show normalized phase space plots of the beam characterized by a given time during the extraction cycle. These plots are essentially "snapshots" of the beam typically made by recording the position and angle of each particle through the last 4 or 5 orbits immediately prior to the time in the cycle shown in the top left-hand corner of each plot. For the purposes of these plots the dipole fields contain only the design harmonics as given in the appendix of the Design Report. The scale factor, shown in the top left of each plot, is 5 mm per division. The other parameters shown refer to the total integrated field

strength of the slow extraction quadrupoles, octopoles, and fast quadrupoles together with the machine chromaticity, horizontal tune, electrostatic septum offset (mms), and the effective septum kick (mrads). Figure 5(d) shows clearly the circulating and extracted beams separated by ~3.5 mms.

Having established the extracted beam phase space behavior for dipoles with the design fields only, we then added the lower four skew harmonics to the dipole fields. This was done by generating random skew coefficients in a gaussian form defined by:

$$a_1 = 1.0 \pm 3.6 \times 10^{-4}$$
$$a_2 = -1.15 \pm 1.5 \times 10^{-4}$$
$$a_3 = -0.6 \pm 2.25 \times 10^{-4}$$
$$a_4 = -0.35 \pm 0.5 \times 10^{-4}$$

(The units are inverse inches)

Unless otherwise stated these harmonic coefficients are used throughout this report. No attempt was made to optimize the distributions to avoid groups of "bad" magnets, likewise we made no cutoffs on the tails of the distributions. Skew fields in the dipoles will have the effect of coupling the horizontal and vertical orbits causing a rapid blowup of the vertical phase space. This effect is demonstrated in Fig. 6 where we have plotted both the vertical (A and C) and horizontal (B and D) phase space at the magnetic septa at 0.1 msec and 0.3 msec into the cycle. Note that the scale for the vertical phase space plots has been changed to 1 mm/div to provide better resolution. It is apparent that after only 0.1 ms (5 revolutions) that the amplitude of the vertical oscillations are the same as the horizontal, i.e., the orbits are fully coupled. The phase of the horizontal oscillations [Fig. 6(d)] has changed by $\pi/2$ from the design value [Fig. 5(d)] and further into the cycle the whole system becomes unstable.

In order to prevent this beam blow up, we installed skew quadrupole correction elements at each normal cell defocussing quadrupole (90 elements). This distribution of correction elements is almost certainly not the optimal one (see, for example, Ohnuma TM-766) but should be sufficiently close to it to get a good idea of the dynamics of the system. With this distribution of correction elements we then adjusted the strength to minimize the amplitude of the vertical oscillations. The results of this procedure are shown in Fig. 7. With the skew quadrupoles running at 10 kG-in. at 1 in. (900 kG-in. total field strength) one can see that the vertical phase space does not change appreciably during the cycle; the maximum amplitude at the Lambertson magnets staying at ~2.0 mms (~3.5 mms at β = 100 ms). This 900 kG-in. for the total integrated field strength of the correction elements is consistent with what one would expect based on the assumption that the integrated strength of the correction elements should be more or less equal to the integrated strength of the dipole skew harmonics for orbit amplitudes of up to 20 mms.

A comparison of these data with that of Fig. 5 shows that controlling the vertical amplitudes to these levels allows the horizontal dynamics to be essentially unchanged. The sensitivity of extraction to this skew field cancellation is demonstrated in Fig. 8 where we mistuned the correction elements by 20%. The beam is still extracted but the vertical amplitude has increased from 2.0 mm to 3.0 mm and shows a definite phase, the horizontal phase space is also beginning to be affected by the skew fields.

The residual skew fields left after this partial cancellation correspond to $a_1 \simeq 2.0 \times 10^{-5}$ hence we conclude that this is the upper bound for skew fields that extraction can tolerate.

We have also looked to see whether the addition of correction octopoles can help to minimize the orbit couplings. We found that with the skew quadrupoles correctly adjusted then there was no noticeable effect when we included skew octopoles. The reason for this is that skew quadrupoles alone are sufficient to approximate the effect of all the skew harmonics provided the orbit amplitudes remain within the ~20 mm range.

The results shown in Fig. 9 are an attempt to see whether or not the correction system is sensitive to the magnitude of the systematic dipole skew quadrupole term. We increased the lower skew coefficient to $a_1 = 3.0 \pm 3.6$ and adjusted the correction elements accordingly. With each element running at 30 kG-in. at 1 in. then the extraction dynamics remain essentially unchanged although the orbit coupling is now sufficiently strong to create a small 1 mm vertical offset [Fig. 9(h)] on the extracted beam. From this we conclude that we are not overtly sensitive to the magnitude of the a_1 coefficient and that with the current magnet selection criteria the correction coil package should be able to successfully eliminate the unwanted harmonics.

So far in this report we have restricted ourselves to considering a machine which possesses the so-called natural chromaticity of -22.5. The correction coil sextupoles as outlined in the Design Report are capable of changing the chromaticity over a large range and in view of this fact we have looked at the effect of chromaticity on extraction. Figure 10 shows the horizontal phase space during extraction with the chromaticity "reversed" to +22.5. Comparing these results with Fig. 5, it is evident that we have increased the separation between the circulating and extracted beam as well

as significantly reducing the phase space area of the extracted beam. There are two main reasons for this behavior.

For a machine with a non-zero chromaticity then the inherent momentum spread of the beam implies an equivalent tune spread. During the extraction cycle, where the tune is moved toward the one-half integer stopband to initiate extraction, then particles of such momenta as to be nearer in tune to the one-half integer will be extracted before those of lower tunes. The proposed layout of extraction devices in the Tevatron has the pulsed fast extraction quadrupoles in the warm 48 mini-straight sections, approximately 20° out of phase with the slow extraction devices in the 28 and 42 locations. As the fast quadrupoles are pulsed then the phase of the separatrix will start to rotate anticlockwise up to a maximum of $\sim 10^\circ$. Particles of a higher tune will be extracted earlier in the cycle when the strength of the fast quadrupoles is relatively small and consequently the phase of the separatrix will be essentially the same as for slow extraction. Particles of a lower tune will be extracted later in the cycle when the field of the fast quadrupoles is greater and therefore will be rotated somewhat in phase. The effect of this phase rotation can be most easily illustrated by considering just two particles A and B with momentum offsets $\pm\Delta p/p$. Ignoring the octopoles for the sake of simplicity then the separatrices for the two particles look like the drawing at the top of the next page. In that picture with a negative machine chromaticity then particle B will be extracted first with little phase space rotation whereas the separatrix for particle A will be rotated away from B, as shown above, causing an increase in the allowable phase space area and a

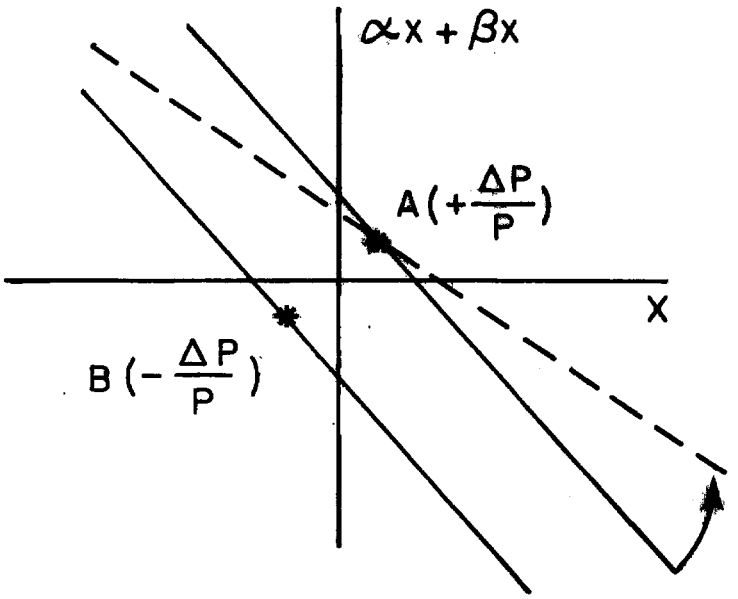

consequent increase in the extracted beam phase space. If we now reverse the machine chromaticity then the trajectory of particle A will remain unchanged but trajectory B will be rotated towards that of particle A causing a decrease in phase space in the extracted beam region. This kind of wedge-shaped phase space is reasonably apparent in Figs. 5 and 10 with the direction of the wedge changing with chromaticity. There is, however, another quite important effect taking place, again associated with momentum which also changes the extracted beam phase space. Once more ignoring octopoles to simplify matters, then the size of the extracted beam, as well as the extraction losses, is strongly affected by the so-called step size across the electrostatic septum. This step size is determined by the strength of the quadrupole 39th harmonic and the septum offset from the closed orbit. In the Tevatron the electrostatic septum is located radially inwards with an 11 mm offset from the on-momentum closed orbit. If we again consider just two

particles with momentum offsets $\pm\Delta p/p$ then looking downstream onto the septum we get

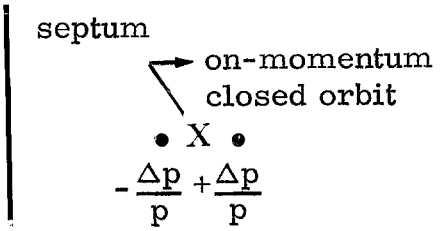

where the off-momentum closed-orbits position the lower momentum particle closer to the septum than the higher momentum one. Because the septum offset appears to be less to the lower momentum particle then the step size, which is proportional to this offset, will be reduced accordingly. With a negative machine chromaticity then the lower momentum particle will have a higher tune and will get extracted earlier in the cycle. At an earlier point in the cycle the relative strength of the fast quadrupoles is less which reduces the step size compared to a later time in the cycle. If we change the machine chromaticity the relative offsets of the electrostatic septum from the off-momentum closed orbits do not change noticeably, but the particles nearer the septum are now extracted when the 39th harmonic quadrupole term is relatively large, which permits a more uniform step-size from all momentum components during the cycle. In conclusion then we can say that a positive machine chromaticity provides a more uniform extracted beam spot as well as smaller phase space area and consequently should be considered the preferred chromaticity for extraction purposes.

The sensitivity of the extracted beam to overall changes in beam momenta is shown in Figs. 11 and 12 where we have changed the overall beam momentum by $\pm 0.025\%$.

An overall change in beam momentum will produce a radial offset in the beam position which in the presence of skew fields (and correction coils) might have been expected to introduce a stronger orbit coupling than in the on-momentum case. This did not prove to be the case, however, and we found no noticeable change in the vertical phase space from that shown in Fig. 7. We therefore conclude that the effect of the correction skew quadrupoles are unaffected by changes in the beam momentum within this range. The changes in phase space between Figs. 11 and 12 are all consistent with being produced by the effective change in septum offset and different spill times.

In the final section of this report we have attempted to simulate our "best guess" machine by using the measured field harmonics on the accepted Tevatron dipoles to generate distributions of dipoles possessing not only skew harmonics but also random lower order normal harmonics too. The normal harmonics were generated according to

$$b_1 = 0 \pm 2.0$$
$$b_2 = 0 \pm 3.0 \qquad \text{(The units are inverse inches)}$$
$$b_3 = -0.3 \pm 1.0$$
$$b_4 = 1.4 \pm 2.0.$$

The higher order normal harmonics were given their design values. We removed the systematic term from the lower two harmonics rather than install correction elements to do this, both approaches are essentially equivalent. Figures 13-15 show the horizontal phase space for three different random distributions of dipoles. The only adjustment made between the different cases was to change the horizontal tune to equalize the spill

time. The overall extraction dynamics are basically similar for all three cases; however, not too surprisingly, the extracted phase space has been diluted by the random fields (c.f., Fig. 10). As we have removed the systematic terms from the b_1 and b_2 coefficients it is presumably reasonable to suppose that harmonics of higher order than the zeroth harmonic are contributing strongly. The next step, which we have not done yet, is to produce a series of correction elements, driving the individual dominant harmonics to provide the necessary fine tuning.

To conclude then we can say that we have demonstrated that skew quadrupole correction elements are capable of controlling orbit coupling to a tolerable level during extraction. With the proposed layout of extraction devices (and any other that involves a septum radially inwards) a positive chromaticity is preferred, and finally we see no undue sensitivity of extraction to off-momentum orbits and the lower order normal dipole harmonics.

I would like to thank Don Edwards for many helpful discussions and comments on the contents of this report.

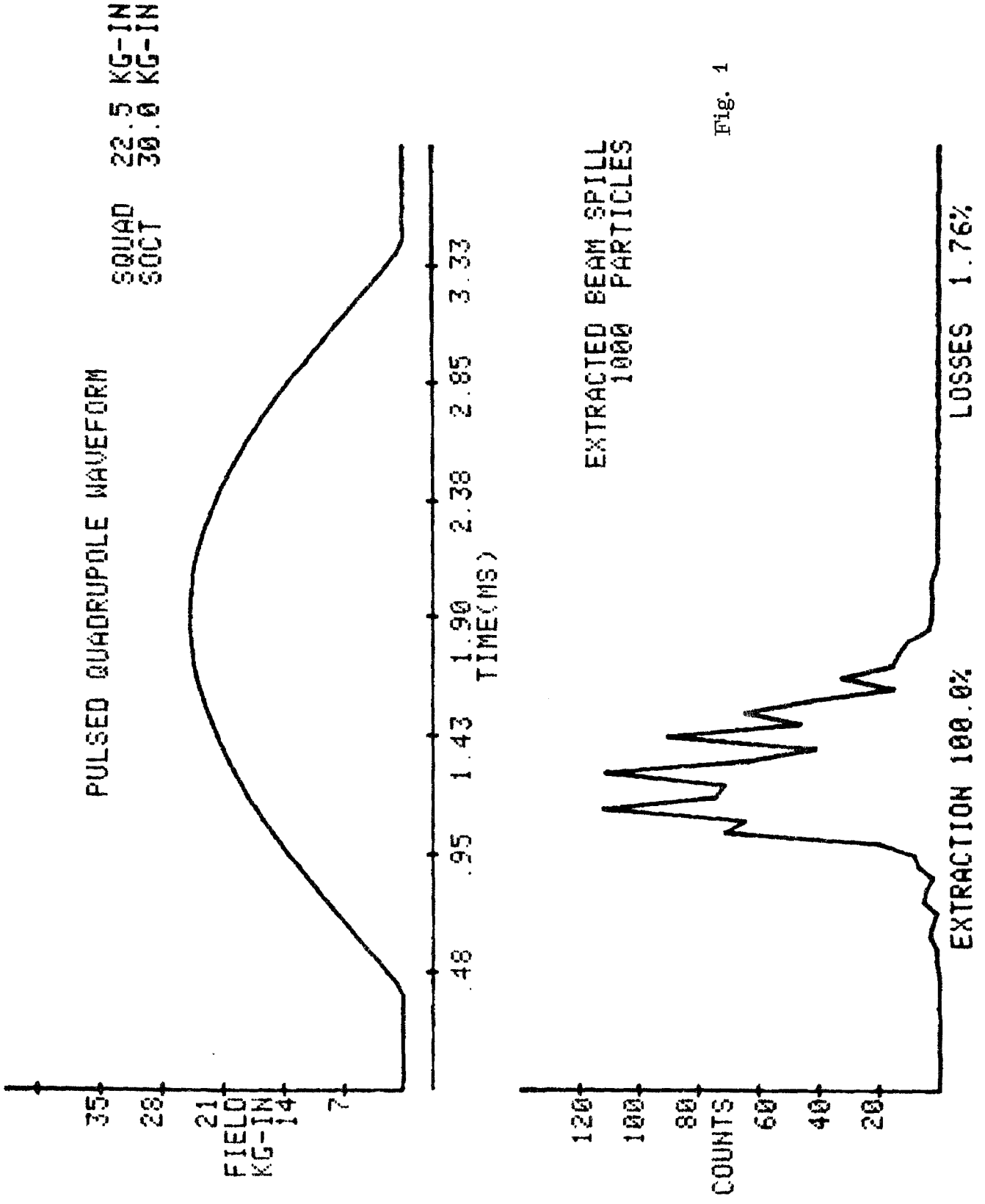
PULSED QUADRUPOLE WAVEFORM
SQUAD 22.5 KG-IN
SOCT 30.0 KG-IN
FIELD KG-IN
35
28
21
14
7
.48
.95
1.43
1.90
2.38
2.85
3.33
TIME(MS)
EXTRACTED BEAM SPILL
1000 PARTICLES
COUNTS
120
100
80
60
40
20
EXTRACTION 100.0%
LOSSES 1.76%

Fig. 1

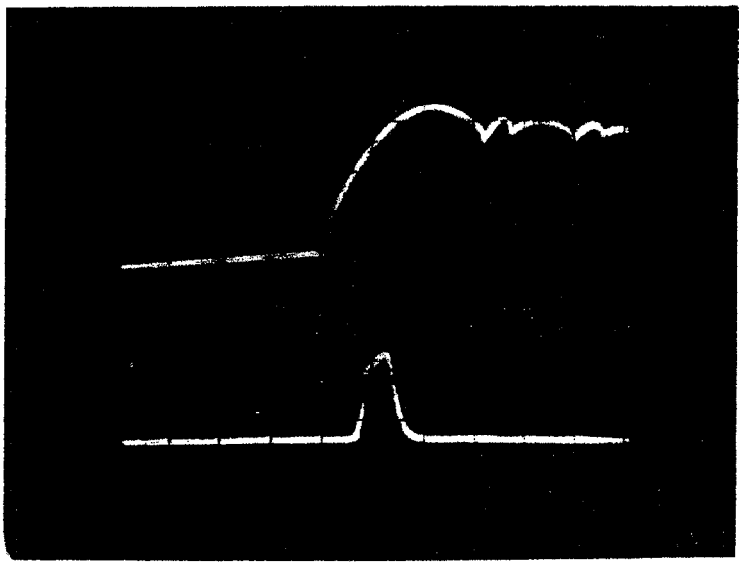

Fig. 2

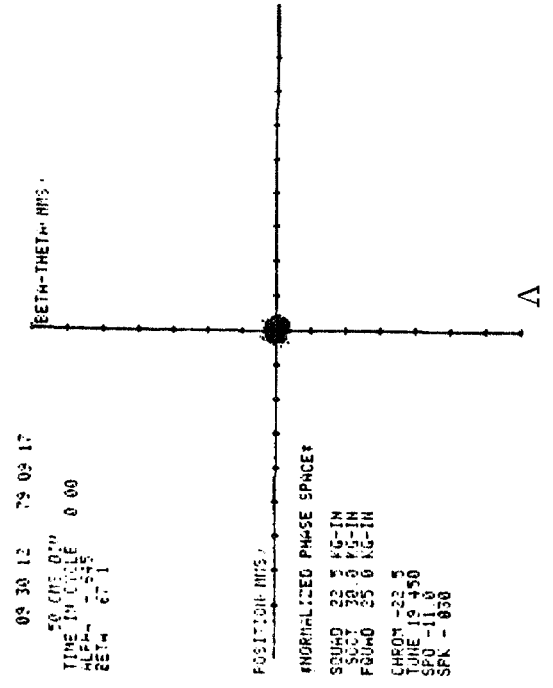
09 30 12 79 09 17
50 CMS 0'0"
TIME IN CYCLE 0 00
#NORMALIZED PHASE SPACE#
SQUAD 22 5 KG-IN
SEXT 30 0 KG-IN
FQUAD 25 0 KG-IN
CHROM -22 5
TUNE 19 450
SPO -11 0
SPK -0 830

A

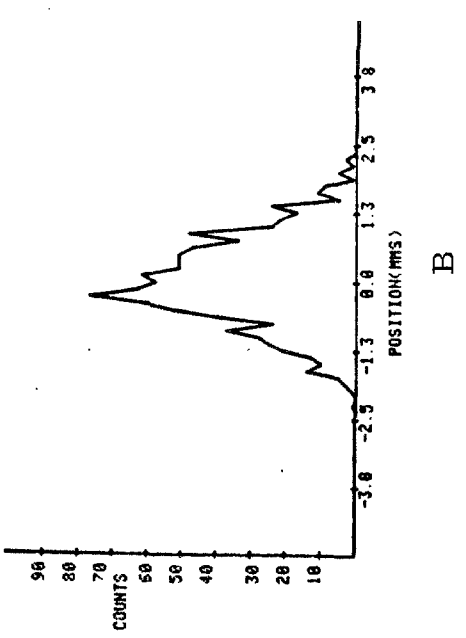
SPATIAL DISTRIBUTION
COUNTS
POSITION(MMS)

B

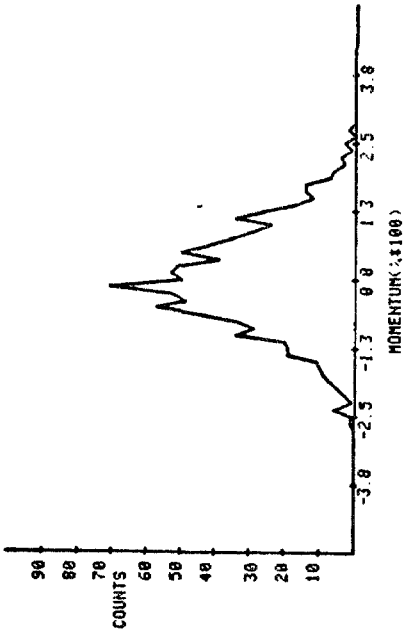
MOMENTUM DISTRIBUTION
COUNTS
MOMENTUM(*100)

C

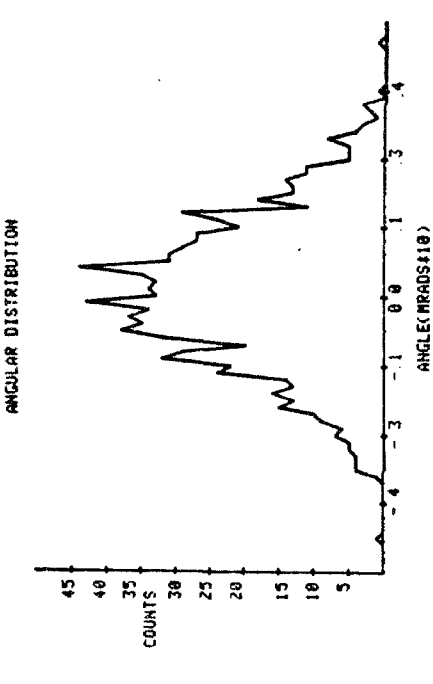
ANGULAR DISTRIBUTION
COUNTS
ANGLE(MRADS*10)

C

Fig. 3

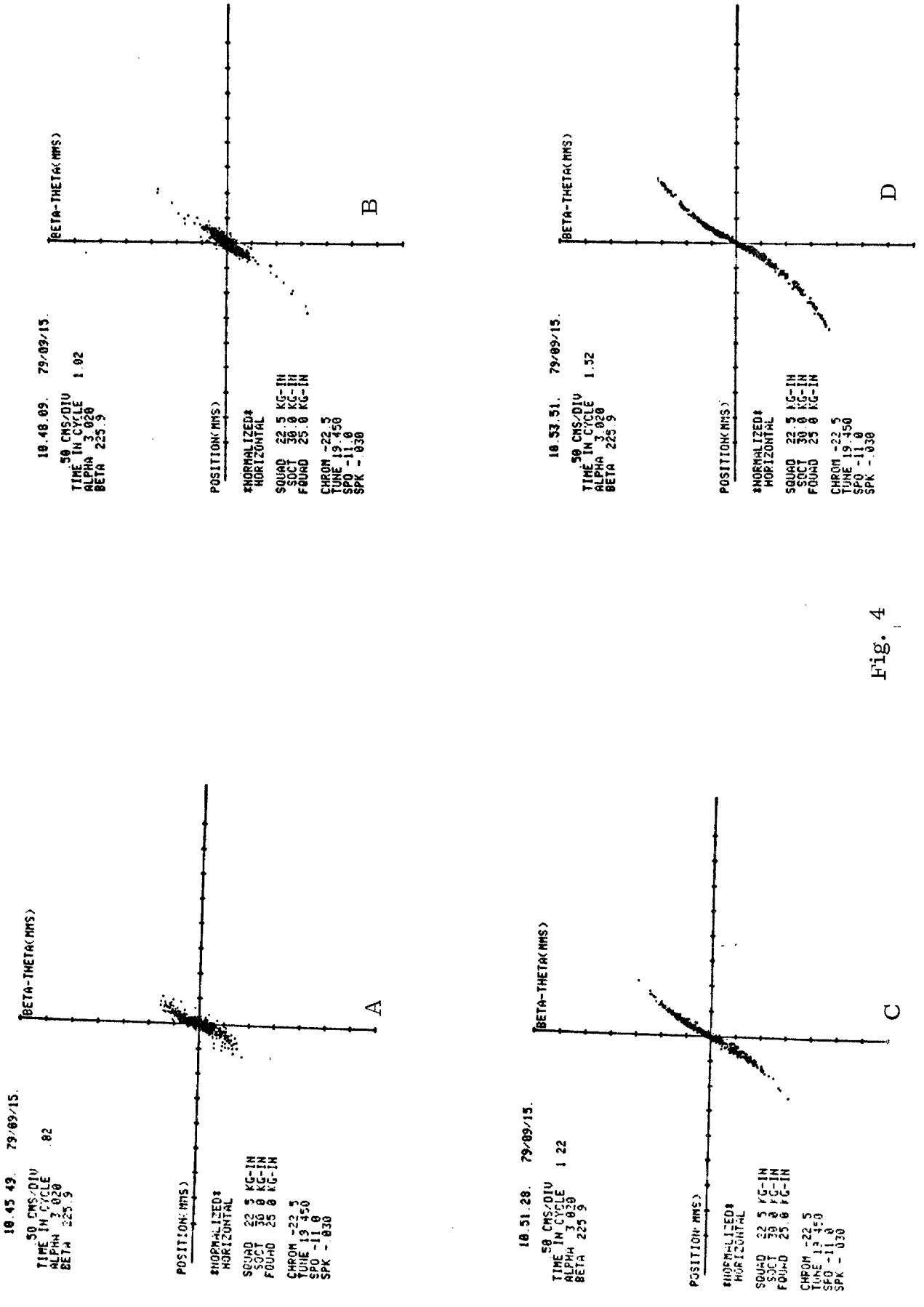
10.45.49. 79/09/15.
50 CMS/DIV
TIME IN CYCLE .82
ALPHA 3.020
BETA 225.9
BETA-THETA(MMS)
POSITION(MMS)
NORMALIZED
HORIZONTAL
SQUAD 22.5 KG-IN
SOCT 30.0 KG-IN
FQUAD 25.0 KG-IN
CHROM -22.5
TUNE 19.450
SPO -11.0
SPK - .030
A
10.48.09. 79/09/15.
50 CMS/DIV
TIME IN CYCLE 1.02
ALPHA 3.020
BETA 225.9
BETA-THETA(MMS)
POSITION(MMS)
NORMALIZED
HORIZONTAL
SQUAD 22.5 KG-IN
SOCT 30.0 KG-IN
FQUAD 25.0 KG-IN
CHROM -22.5
TUNE 19.450
SPO -11.0
SPK - .030
B
10.51.28. 79/09/15.
50 CMS/DIV
TIME IN CYCLE 1.22
ALPHA 3.020
BETA 225.9
BETA-THETA(MMS)
POSITION(MMS)
NORMALIZED
HORIZONTAL
SQUAD 22.5 KG-IN
SOCT 30.0 KG-IN
FQUAD 25.0 KG-IN
CHROM -22.5
TUNE 19.450
SPO -11.0
SPK - .030
C
10.53.51. 79/09/15.
50 CMS/DIV
TIME IN CYCLE 1.42
ALPHA 3.020
BETA 225.9
BETA-THETA(MMS)
POSITION(MMS)
NORMALIZED
HORIZONTAL
SQUAD 22.5 KG-IN
SOCT 30.0 KG-IN
FQUAD 25.0 KG-IN
CHROM -22.5
TUNE 19.450
SPO -11.0
SPK - .030
D

Fig. 4

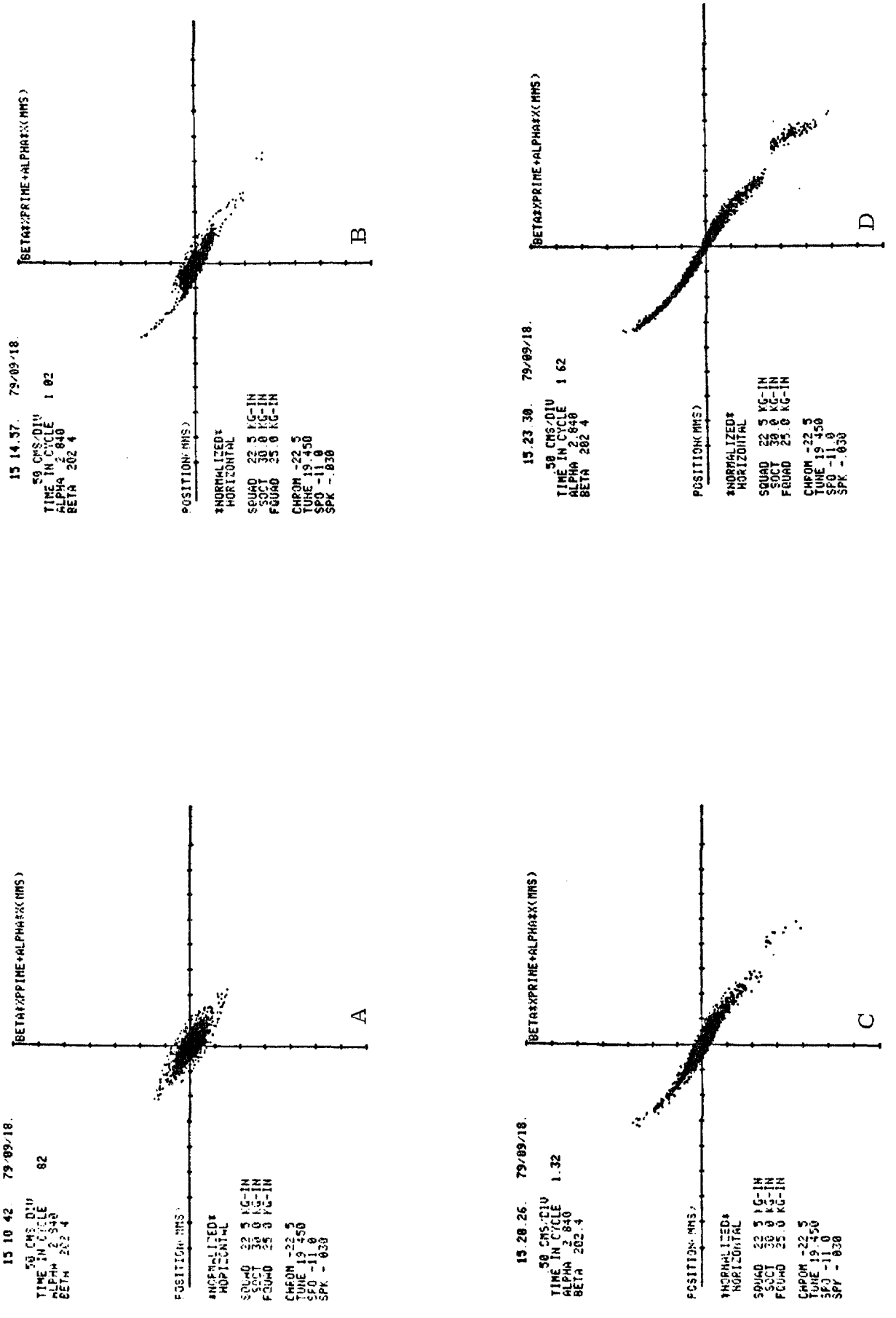
15 10 42 79/09/18.
50 CMS/DIV
TIME IN CYCLE 82
ALPHA 2.840
BETA 282.4
BETAXPRIME+ALPHA*X(MMS)
POSITION(MMS)
NORMALIZED
HORIZONTAL
SQUAD 22.5 KG-IN
SQCT 30.0 KG-IN
FQUAD 25.0 KG-IN
CMPOM -22.5
TUNE 19.450
SPO -11.0
SPK -.030
A
15 14 57. 79/09/18.
50 CMS/DIV
TIME IN CYCLE 1.02
ALPHA 2.840
BETA 282.4
BETAXPRIME+ALPHA*X(MMS)
POSITION(MMS)
NORMALIZED
HORIZONTAL
SQUAD 22.5 KG-IN
SQCT 30.0 KG-IN
FQUAD 25.0 KG-IN
CMPOM -22.5
TUNE 19.450
SPO -11.0
SPK -.030
B
15 20 26. 79/09/18.
50 CMS/DIV
TIME IN CYCLE 1.32
ALPHA 2.840
BETA 282.4
BETAXPRIME+ALPHA*X(MMS)
POSITION(MMS)
NORMALIZED
HORIZONTAL
SQUAD 22.5 KG-IN
SQCT 30.0 KG-IN
FQUAD 25.0 KG-IN
CMPOM -22.5
TUNE 19.450
SPO -11.0
SPK -.030
C
15 23 30. 79/09/18.
50 CMS/DIV
TIME IN CYCLE 1.62
ALPHA 2.840
BETA 282.4
BETAXPRIME+ALPHA*X(MMS)
POSITION(MMS)
NORMALIZED
HORIZONTAL
SQUAD 22.5 KG-IN
SQCT 30.0 KG-IN
FQUAD 25.0 KG-IN
CMPOM -22.5
TUNE 19.450
SPO -11.0
SPK -.030
D

Fig. 5

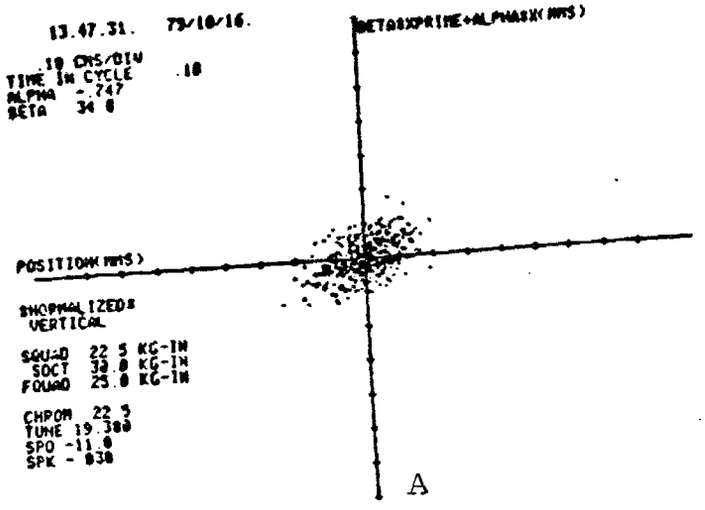
13.47.31. 79/10/16.
.10 CMS/DIV
TIME IN CYCLE .10
ALPHA -.747
BETA 34.0
BETA$XPRIME+ALPHA$X(MMS)
POSITION(MMS)
$NORMALIZED$
VERTICAL
SQUAD 22.5 KG-IN
SOCT 30.0 KG-IN
FQUAD 25.0 KG-IN
CHROM 22.5
TUNE 19.380
SPO -11.0
SPK -.030
A

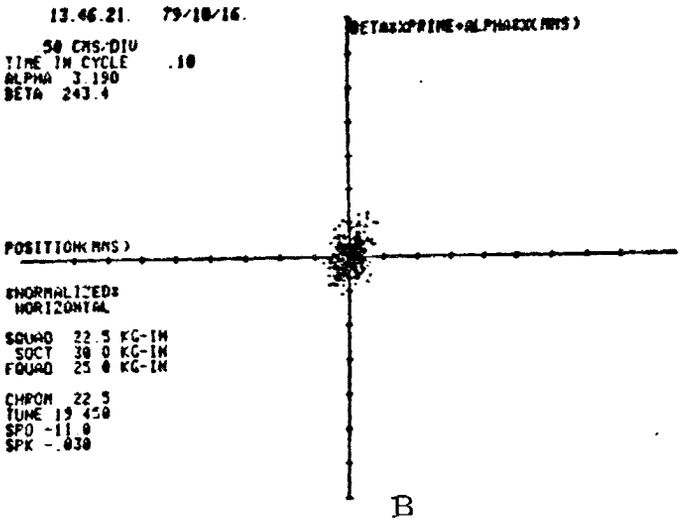
13.46.21. 79/10/16.
.50 CMS/DIV
TIME IN CYCLE .10
ALPHA 3.190
BETA 243.4
BETA$XPRIME+ALPHA$X(MMS)
POSITION(MMS)
$NORMALIZED$
HORIZONTAL
SQUAD 22.5 KG-IN
SOCT 30.0 KG-IN
FQUAD 25.0 KG-IN
CHROM 22.5
TUNE 19.450
SPO -11.0
SPK -.030
B

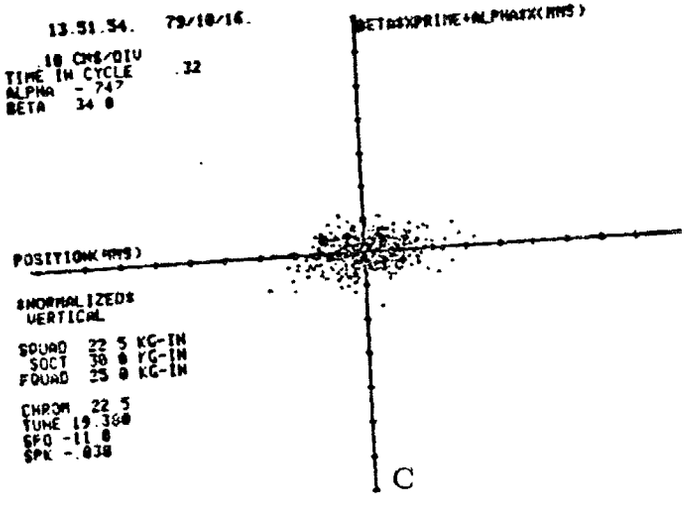
13.51.54. 79/10/16.
.10 CMS/DIV
TIME IN CYCLE .32
ALPHA -.747
BETA 34.0
BETA$XPRIME+ALPHA$X(MMS)
POSITION(MMS)
$NORMALIZED$
VERTICAL
SQUAD 22.5 KG-IN
SOCT 30.0 KG-IN
FQUAD 25.0 KG-IN
CHROM 22.5
TUNE 19.380
SPO -11.0
SPK -.030
C

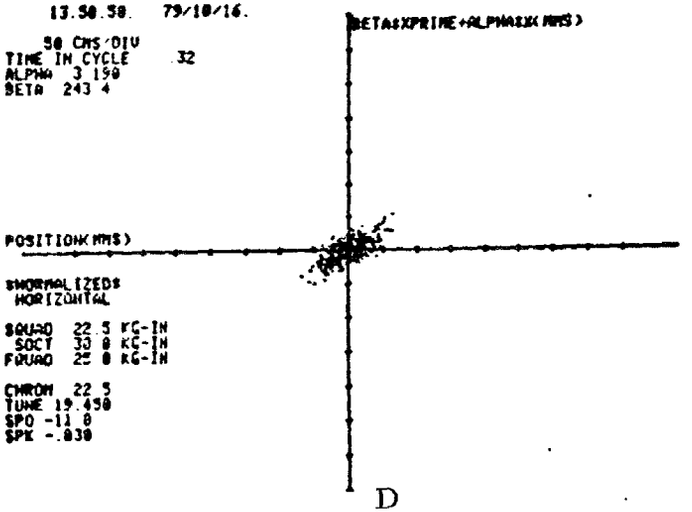
13.50.50. 79/10/16.
.50 CMS/DIV
TIME IN CYCLE .32
ALPHA 3.190
BETA 243.4
BETA$XPRIME+ALPHA$X(MMS)
POSITION(MMS)
$NORMALIZED$
HORIZONTAL
SQUAD 22.5 KG-IN
SOCT 30.0 KG-IN
FQUAD 25.0 KG-IN
CHROM 22.5
TUNE 19.450
SPO -11.0
SPK -.030
D

Fig. 6

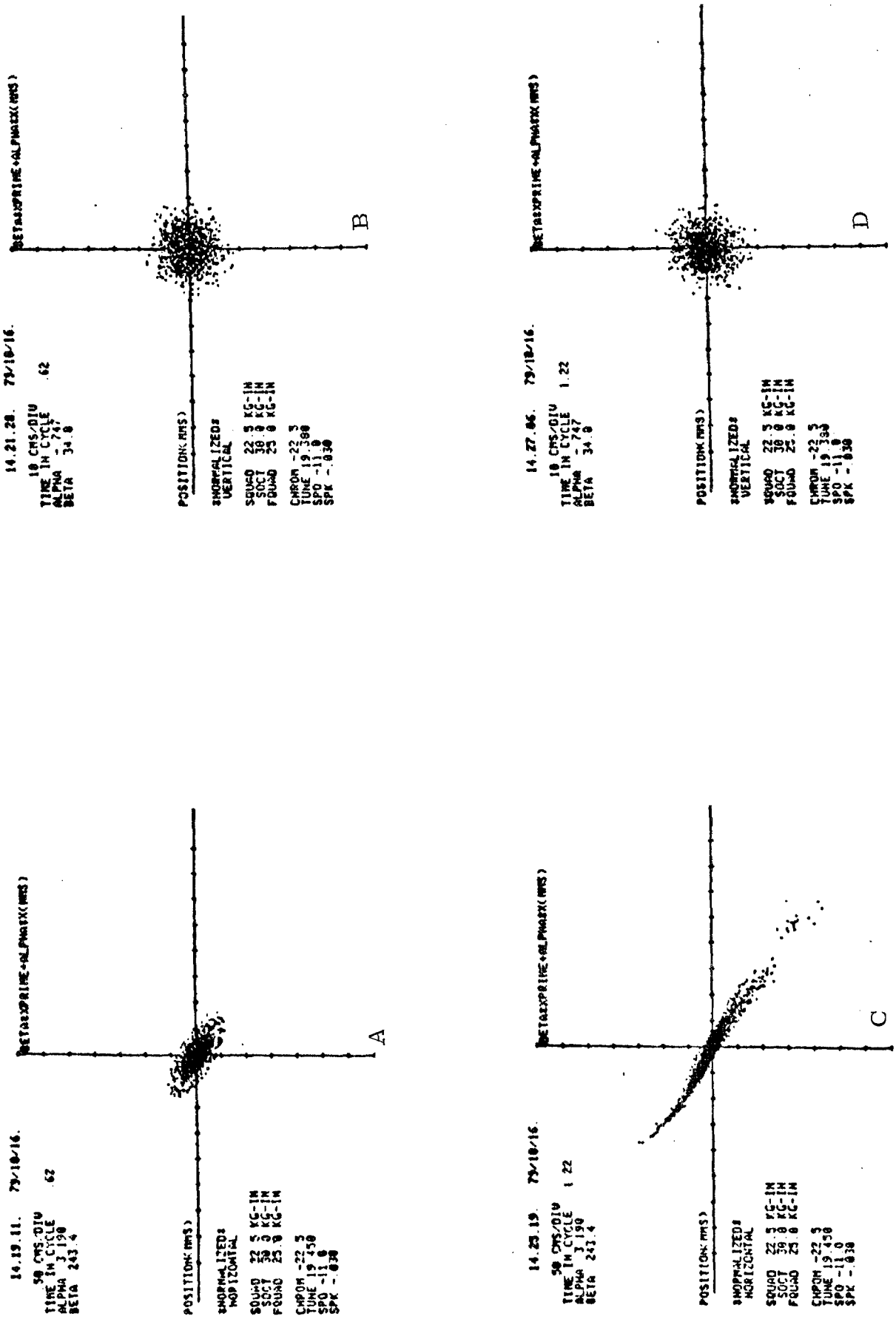
14.19.11. 79/10/16.
50 CMS/DIV .62
TIME IN CYCLE
ALPHA 3.190
BETA 243.4
BETA(SPRIME+ALPHA(RMS)
POSITION(RMS)
ANORMALIZED:
HORIZONTAL
SQUAD 22.5 KG-IN
SOCT 30.0 KG-IN
FQUAD 25.0 KG-IN
CHROM -22.5
TUNE 19.450
SPO -11.0
SPK -.030
A
14.21.28. 79/10/16.
10 CMS/DIV .62
TIME IN CYCLE
ALPHA -.747
BETA 34.0
BETA(SPRIME+ALPHA(RMS)
POSITION(RMS)
ANORMALIZED:
VERTICAL
SQUAD 22.5 KG-IN
SOCT 30.0 KG-IN
FQUAD 25.0 KG-IN
CHROM -22.5
TUNE 19.350
SPO -11.0
SPK -.030
B
14.23.19. 79/10/16.
50 CMS/DIV 1.22
TIME IN CYCLE
ALPHA 3.190
BETA 243.4
BETA(SPRIME+ALPHA(RMS)
POSITION(RMS)
ANORMALIZED:
HORIZONTAL
SQUAD 22.5 KG-IN
SOCT 30.0 KG-IN
FQUAD 25.0 KG-IN
CHROM -22.5
TUNE 19.450
SPO -11.0
SPK -.030
C
14.27.06. 79/10/16.
10 CMS/DIV 1.22
TIME IN CYCLE
ALPHA -.747
BETA 34.0
BETA(SPRIME+ALPHA(RMS)
POSITION(RMS)
ANORMALIZED:
VERTICAL
SQUAD 22.5 KG-IN
SOCT 30.0 KG-IN
FQUAD 25.0 KG-IN
CHROM -22.5
TUNE 19.350
SPO -11.0
SPK -.030
D

Fig. 7

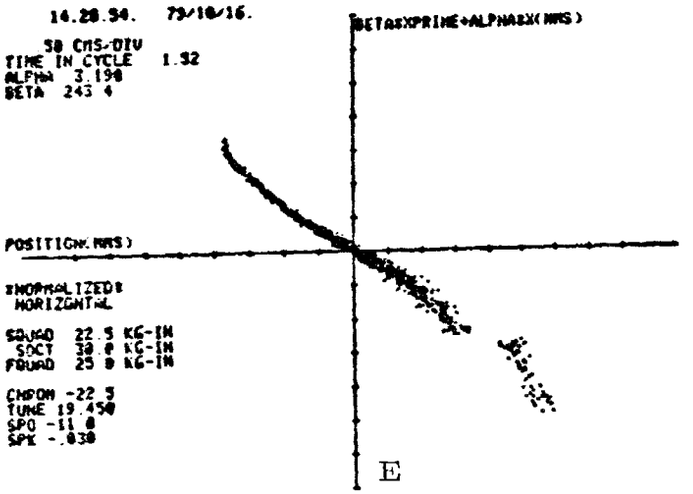

E

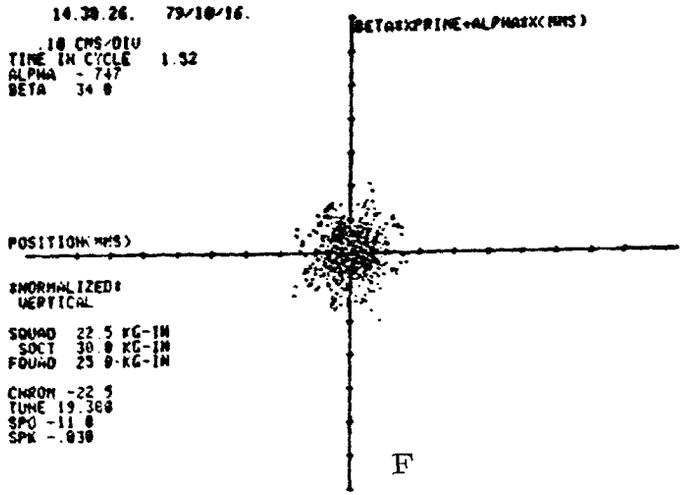

F

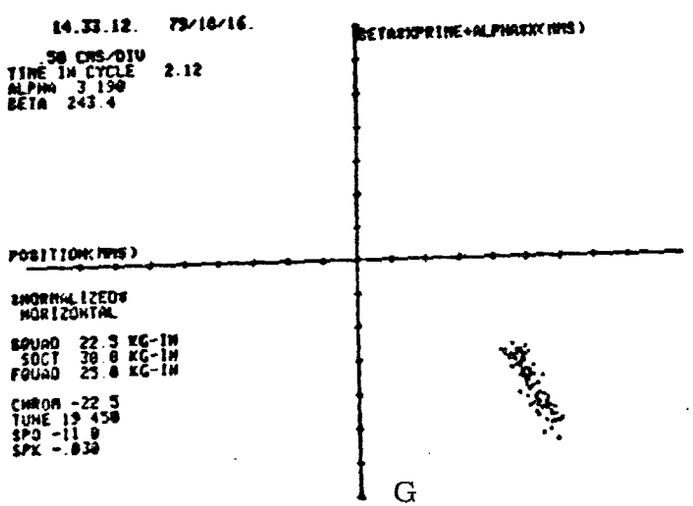

G

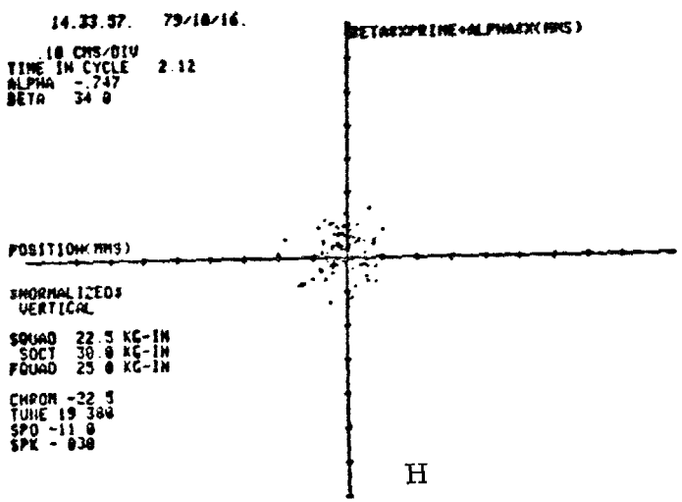

H

Fig. 7 (Cont.)

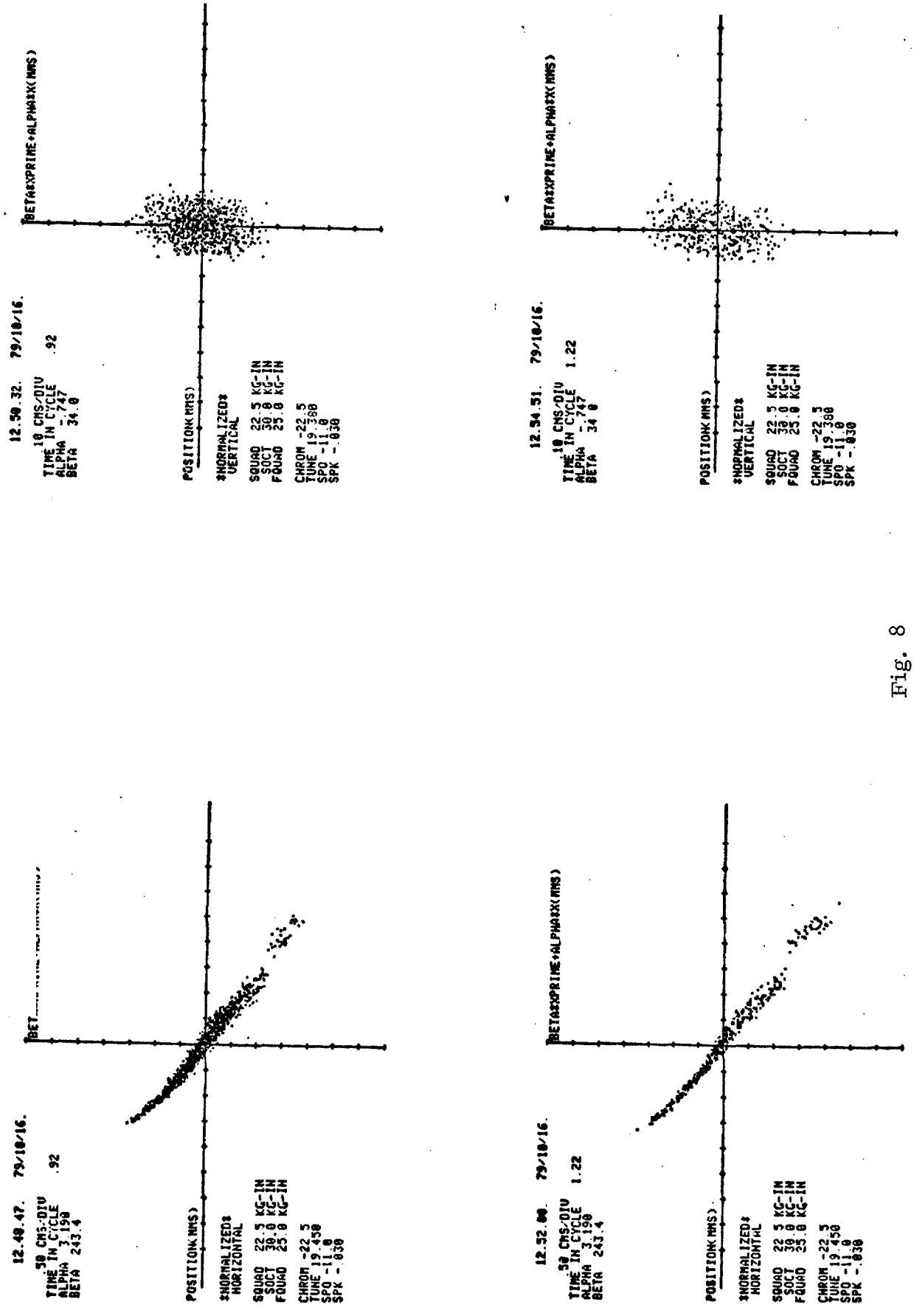
12.50.32. 79/10/16.
10 CMS/DIV
TIME IN CYCLE .92
ALPHA -.747
BETA 34.0
BETAXPRIME+ALPHAXX(MMS)
POSITION(MMS)
NORMALIZED
VERTICAL
SQUAD 22.5 KG-IN
SOCT 30.0 KG-IN
FQUAD 25.0 KG-IN
CHROM -22.5
TUNE 19.388
SPO -11.0
SPK -.030
12.54.51. 79/10/16.
10 CMS/DIV
TIME IN CYCLE 1.22
ALPHA -.747
BETA 34.0
BETAXPRIME+ALPHAXX(MMS)
POSITION(MMS)
NORMALIZED
VERTICAL
SQUAD 22.5 KG-IN
SOCT 30.0 KG-IN
FQUAD 25.0 KG-IN
CHROM -22.5
TUNE 19.388
SPO -11.0
SPK -.030
12.48.47. 79/10/16.
30 CMS/DIV
TIME IN CYCLE .92
ALPHA 3.190
BETA 243.4
BET
POSITION(MMS)
NORMALIZED
HORIZONTAL
SQUAD 22.5 KG-IN
SOCT 30.0 KG-IN
FQUAD 25.0 KG-IN
CHROM -22.5
TUNE 19.450
SPO -11.0
SPK -.030
12.52.00. 79/10/16.
30 CMS/DIV
TIME IN CYCLE 1.22
ALPHA 3.190
BETA 243.4
BETAXPRIME+ALPHAXX(MMS)
POSITION(MMS)
NORMALIZED
HORIZONTAL
SQUAD 22.5 KG-IN
SOCT 30.0 KG-IN
FQUAD 25.0 KG-IN
CHROM -22.5
TUNE 19.450
SPO -11.0
SPK -.030

Fig. 8

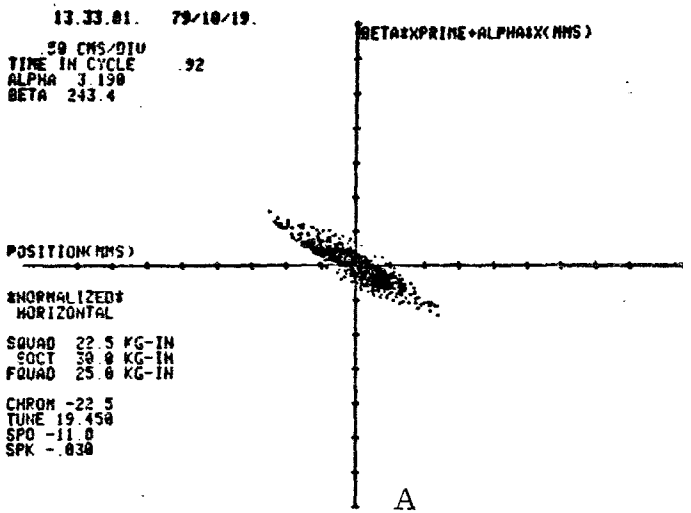
13.33.81. 79/10/19.
.50 CMS/DIV
TIME IN CYCLE .92
ALPHA 3.190
BETA 243.4
BETA*XPRIME+ALPHA*X(MMS)
POSITION(MMS)
NORMALIZED
HORIZONTAL
SQUAD 22.5 KG-IN
SOCT 30.0 KG-IN
FQUAD 25.0 KG-IN
CHROM -22.5
TUNE 19.450
SPO -11.0
SPK -.030

A

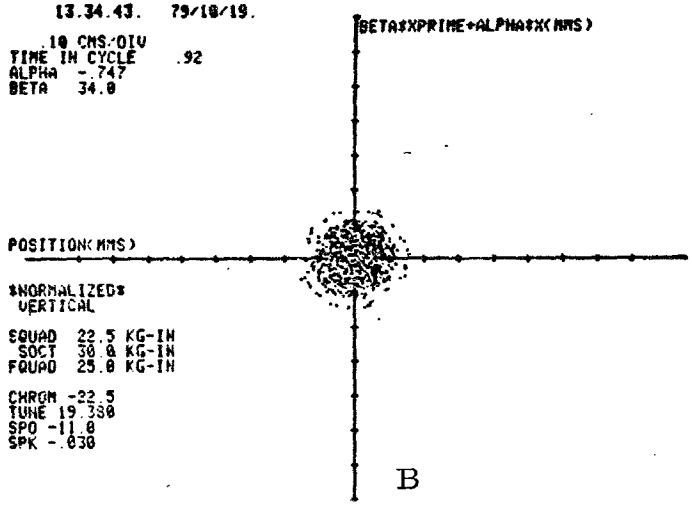
13.34.43. 79/10/19.
.10 CMS/DIV
TIME IN CYCLE .92
ALPHA -.747
BETA 34.0
BETA*XPRIME+ALPHA*X(MMS)
POSITION(MMS)
NORMALIZED
VERTICAL
SQUAD 22.5 KG-IN
SOCT 30.0 KG-IN
FQUAD 25.0 KG-IN
CHROM -22.5
TUNE 19.380
SPO -11.0
SPK -.030

B

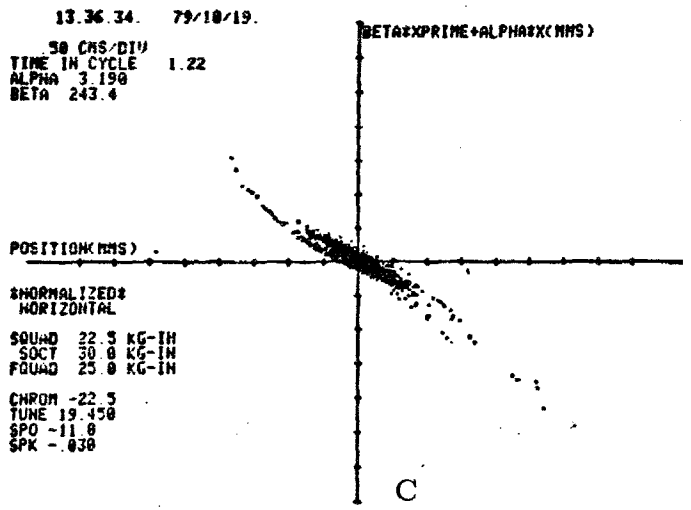
13.36.34. 79/10/19.
.50 CMS/DIV
TIME IN CYCLE 1.22
ALPHA 3.190
BETA 243.4
BETA*XPRIME+ALPHA*X(MMS)
POSITION(MMS)
NORMALIZED
HORIZONTAL
SQUAD 22.5 KG-IN
SOCT 30.0 KG-IN
FQUAD 25.0 KG-IN
CHROM -22.5
TUNE 19.450
SPO -11.0
SPK -.030

C

Fig. 9

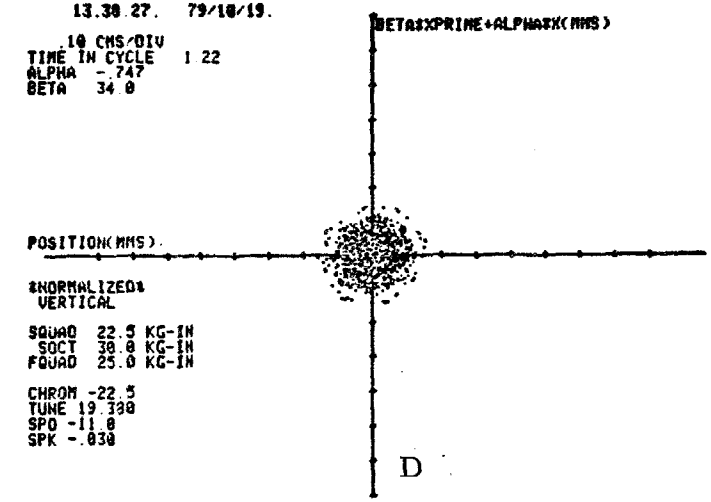
13.38.27. 79/10/19.
.10 CMS/DIV
TIME IN CYCLE 1.22
ALPHA -.747
BETA 34.0
BETA*XPRIME+ALPHA*X(MMS)
POSITION(MMS)
NORMALIZED
VERTICAL
SQUAD 22.5 KG-IN
SOCT 30.0 KG-IN
FQUAD 25.0 KG-IN
CHROM -22.5
TUNE 19.380
SPO -11.0
SPK -.030

D

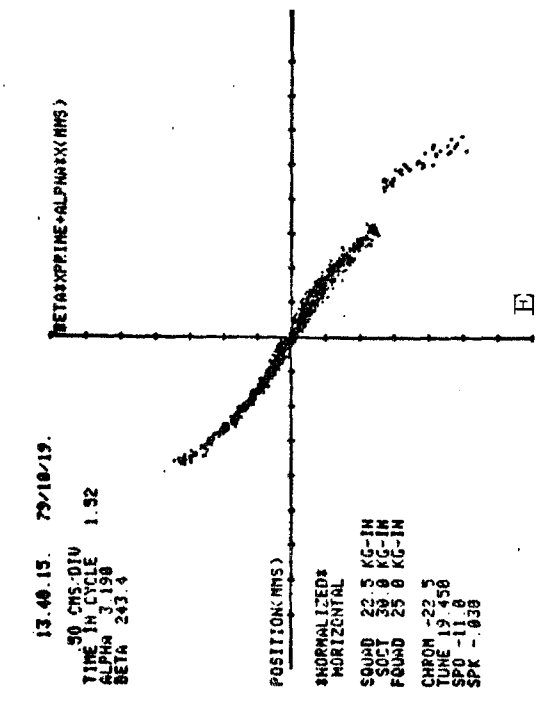

E

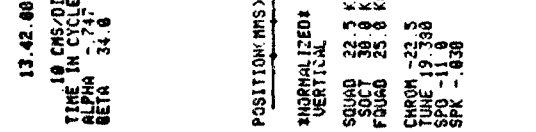

F

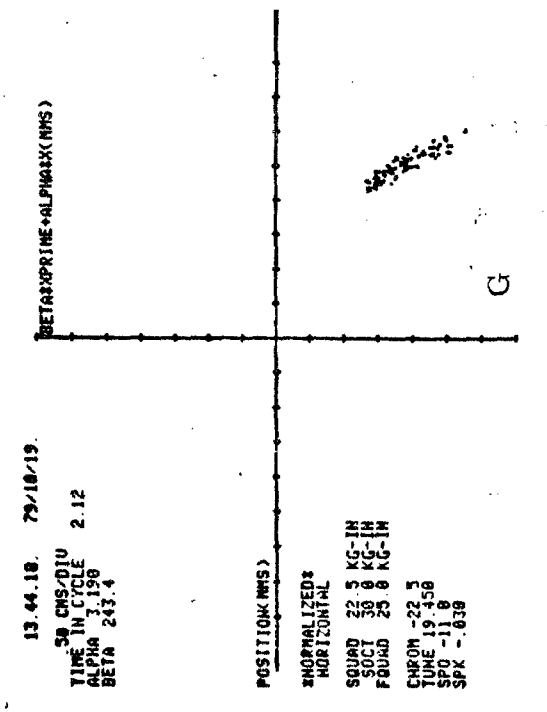

G

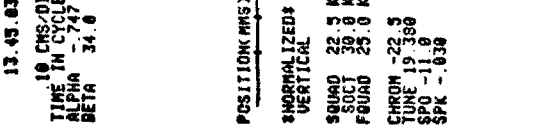

H

Fig. 9
(Cont.)

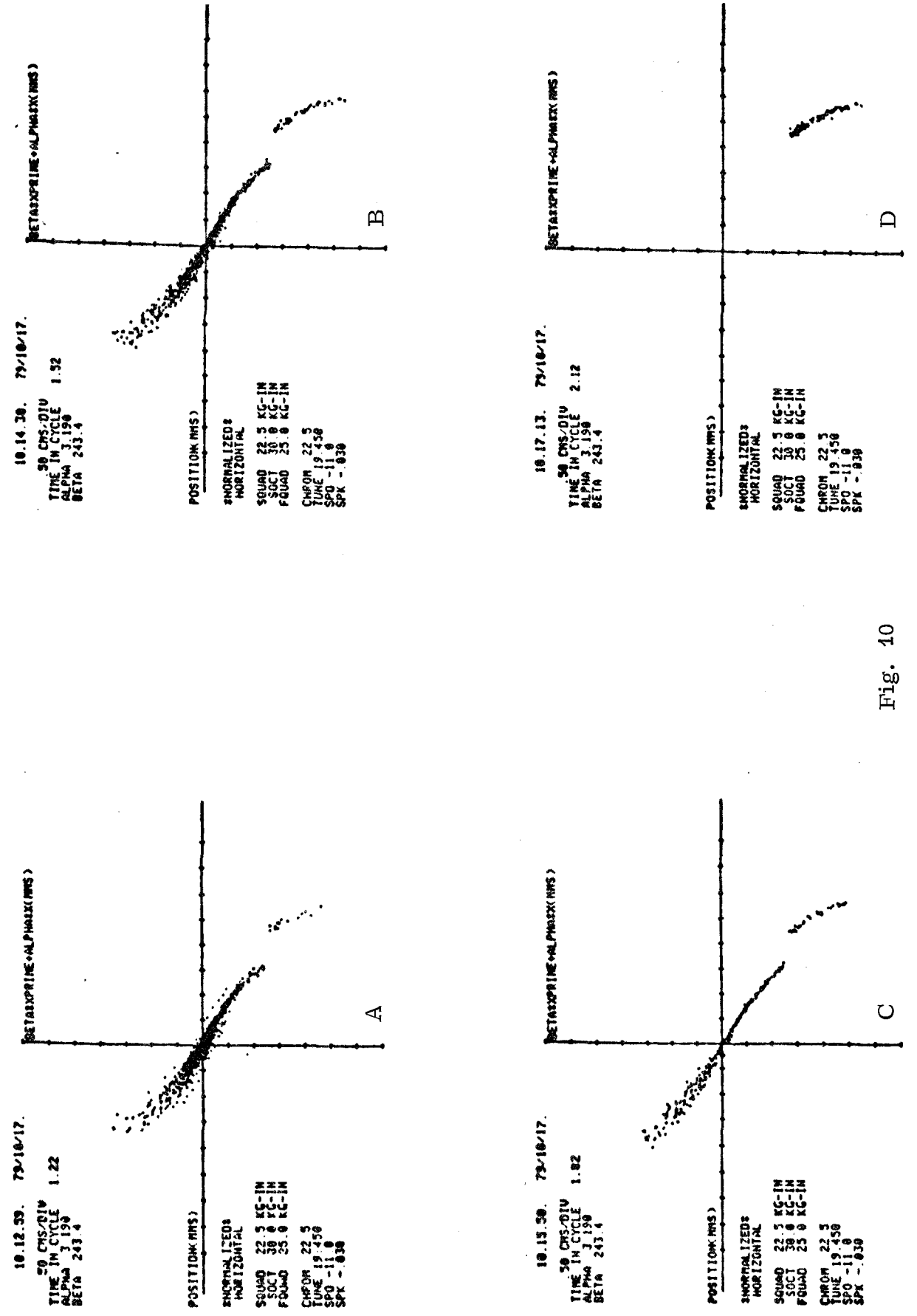
10.12.39. 79/10/17.
50 CMS/DIV
TIME IN CYCLE 1.22
ALPHA 3.190
BETA 243.4
BETAXPRIME+ALPHAX(MMS)
POSITION(MMS)
NORMALIZED:
HORIZONTAL
SQUAD 22.5 KG-IN
SOCT 30.0 KG-IN
FQUAD 25.0 KG-IN
CHROM 22.5
TUNE 19.450
SPO -11.0
SPK -.030
A
10.14.38. 79/10/17.
50 CMS/DIV
TIME IN CYCLE 1.52
ALPHA 3.190
BETA 243.4
BETAXPRIME+ALPHAX(MMS)
POSITION(MMS)
NORMALIZED:
HORIZONTAL
SQUAD 22.5 KG-IN
SOCT 30.0 KG-IN
FQUAD 25.0 KG-IN
CHROM 22.5
TUNE 19.450
SPO -11.0
SPK -.030
B
10.13.58. 79/10/17.
50 CMS/DIV
TIME IN CYCLE 1.82
ALPHA 3.190
BETA 243.4
BETAXPRIME+ALPHAX(MMS)
POSITION(MMS)
NORMALIZED:
HORIZONTAL
SQUAD 22.5 KG-IN
SOCT 30.0 KG-IN
FQUAD 25.0 KG-IN
CHROM 22.5
TUNE 19.450
SPO -11.0
SPK -.030
C
10.17.13. 79/10/17.
50 CMS/DIV
TIME IN CYCLE 2.12
ALPHA 3.190
BETA 243.4
BETAXPRIME+ALPHAX(MMS)
POSITION(MMS)
NORMALIZED:
HORIZONTAL
SQUAD 22.5 KG-IN
SOCT 30.0 KG-IN
FQUAD 25.0 KG-IN
CHROM 22.5
TUNE 19.450
SPO -11.0
SPK -.030
D

Fig. 10

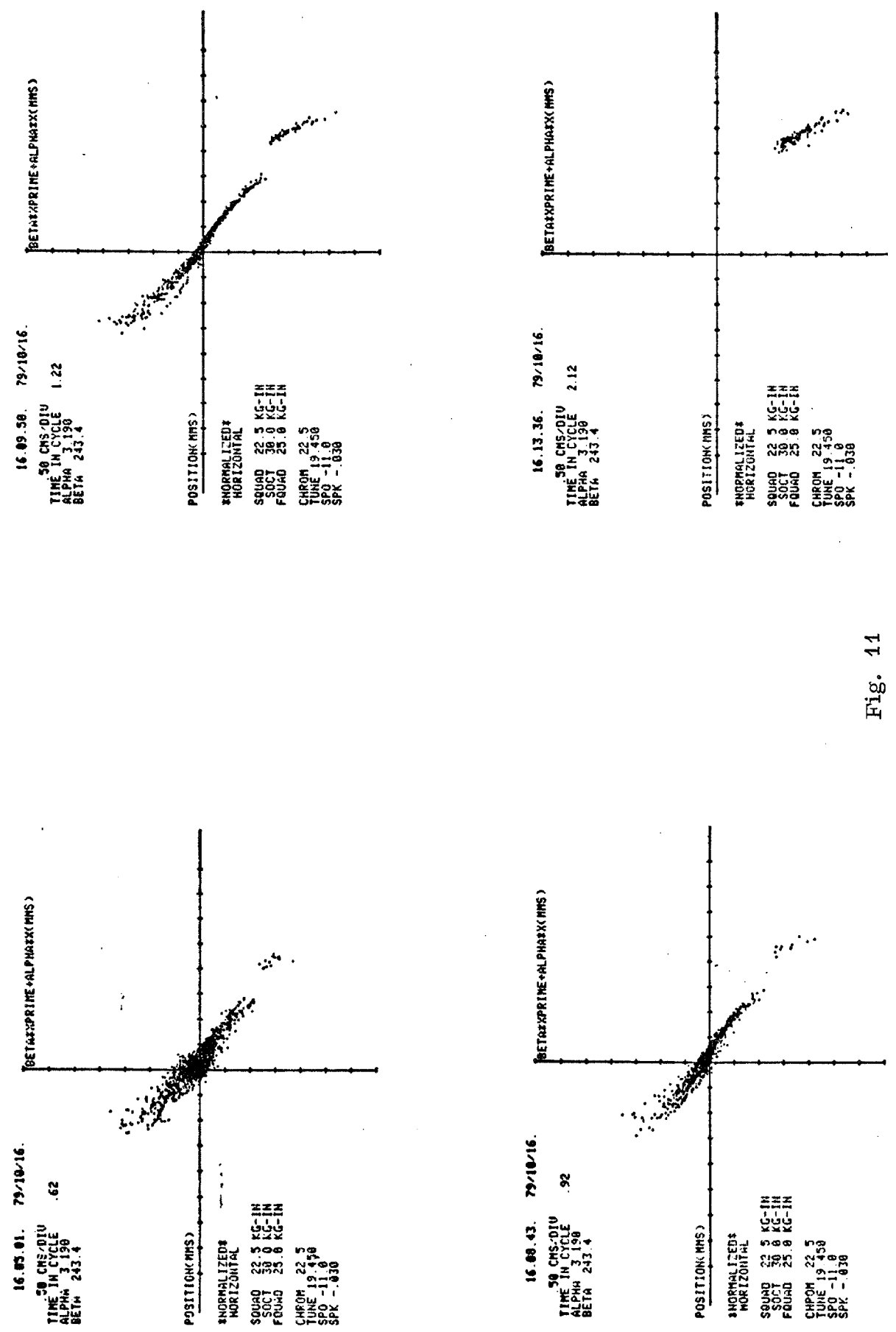
16.09.58. 79/10/16.
50 CMS/DIV
TIME IN CYCLE 1.22
ALPHA 3.190
BETA 243.4
BETAX:PRIME+ALPHAXX(MMS)
POSITION(MMS)
NORMALIZED
HORIZONTAL
SQUAD 22.5 KG-IN
SOCT 30.0 KG-IN
FQUAD 25.0 KG-IN
CHROM 22.5
TUNE 19.450
SPO -11.0
SPK -.030
16.13.36. 79/10/16.
50 CMS/DIV
TIME IN CYCLE 2.12
ALPHA 3.190
BETA 243.4
BETAX:PRIME+ALPHAXX(MMS)
POSITION(MMS)
NORMALIZED
HORIZONTAL
SQUAD 22.5 KG-IN
SOCT 30.0 KG-IN
FQUAD 25.0 KG-IN
CHROM 22.5
TUNE 19.450
SPO -11.0
SPK -.030
16.05.01. 79/10/16.
50 CMS/DIV
TIME IN CYCLE .62
ALPHA 3.190
BETA 243.4
BETAX:PRIME+ALPHAXX(MMS)
POSITION(MMS)
NORMALIZED
HORIZONTAL
SQUAD 22.5 KG-IN
SOCT 30.0 KG-IN
FQUAD 25.0 KG-IN
CHROM 22.5
TUNE 19.450
SPO -11.0
SPK -.030
16.08.43. 79/10/16.
50 CMS/DIV
TIME IN CYCLE .92
ALPHA 3.190
BETA 243.4
BETAX:PRIME+ALPHAXX(MMS)
POSITION(MMS)
NORMALIZED
HORIZONTAL
SQUAD 22.5 KG-IN
SOCT 30.0 KG-IN
FQUAD 25.0 KG-IN
CHROM 22.5
TUNE 19.450
SPO -11.0
SPK -.030

Fig. 11

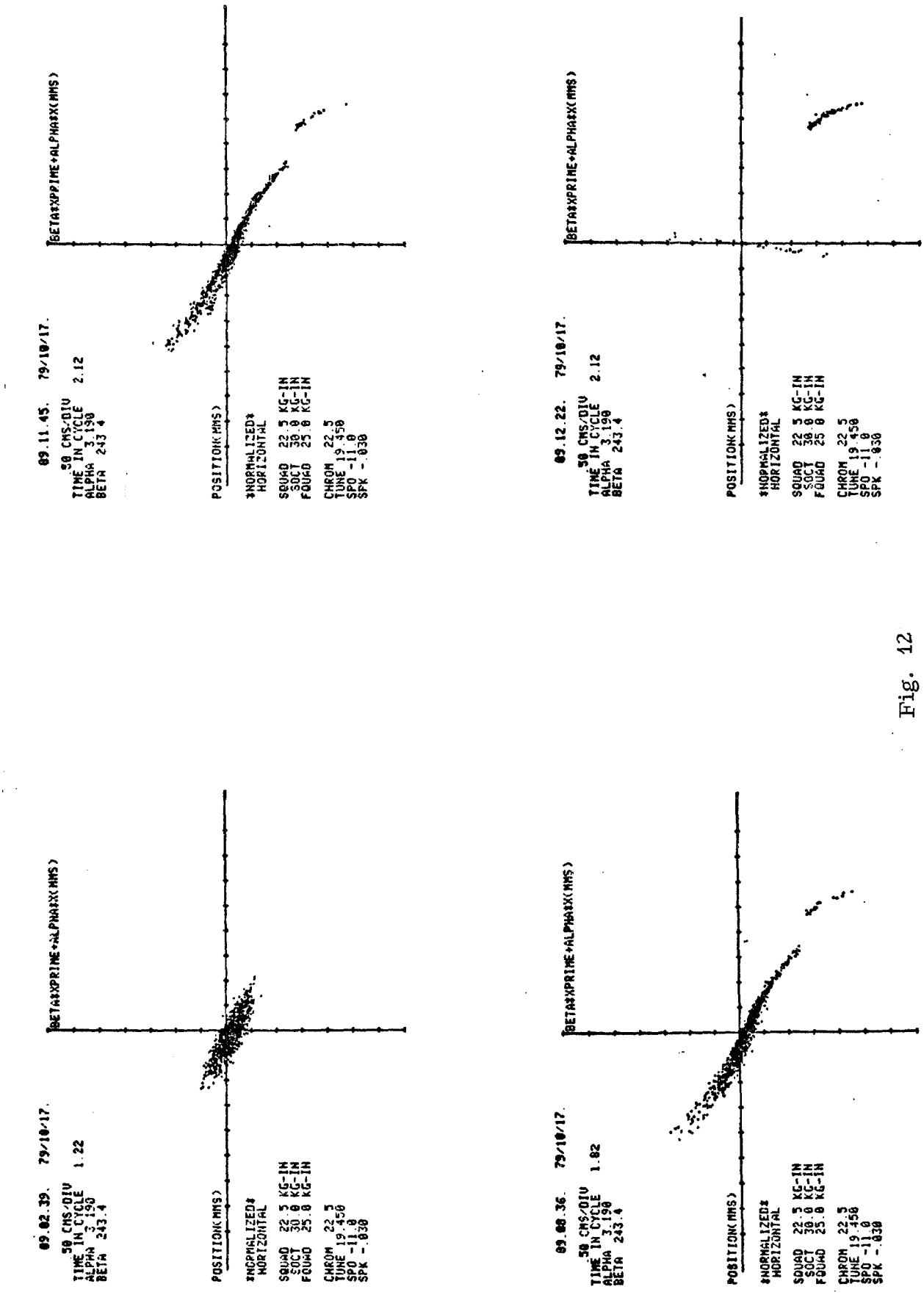
09.11.45. 79/10/17.
50 CMS/DIV
TIME IN CYCLE 2.12
ALPHA 3.190
BETA 243.4
BETAXPRIME+ALPHAX(MMS)
POSITION(MMS)
#NORMALIZED#
HORIZONTAL
SQUAD 22.5 KG-IN
SOCT 30.0 KG-IN
FQUAD 25.0 KG-IN
CHROM 22.5
TUNE 19.450
SPO -11.0
SPK -.030
09.12.22. 79/10/17.
50 CMS/DIV
TIME IN CYCLE 2.12
ALPHA 3.190
BETA 243.4
BETAXPRIME+ALPHAX(MMS)
POSITION(MMS)
#NORMALIZED#
HORIZONTAL
SQUAD 22.5 KG-IN
SOCT 30.0 KG-IN
FQUAD 25.0 KG-IN
CHROM 22.5
TUNE 19.450
SPO -11.0
SPK -.030
09.02.39. 79/10/17.
50 CMS/DIV
TIME IN CYCLE 1.22
ALPHA 3.190
BETA 243.4
BETAXPRIME+ALPHAX(MMS)
POSITION(MMS)
#NORMALIZED#
HORIZONTAL
SQUAD 22.5 KG-IN
SOCT 30.0 KG-IN
FQUAD 25.0 KG-IN
CHROM 22.5
TUNE 19.450
SPO -11.0
SPK -.030
09.00.36. 79/10/17.
50 CMS/DIV
TIME IN CYCLE 1.02
ALPHA 3.190
BETA 243.4
BETAXPRIME+ALPHAX(MMS)
POSITION(MMS)
#NORMALIZED#
HORIZONTAL
SQUAD 22.5 KG-IN
SOCT 30.0 KG-IN
FQUAD 25.0 KG-IN
CHROM 22.5
TUNE 19.450
SPO -11.0
SPK -.030

Fig. 12

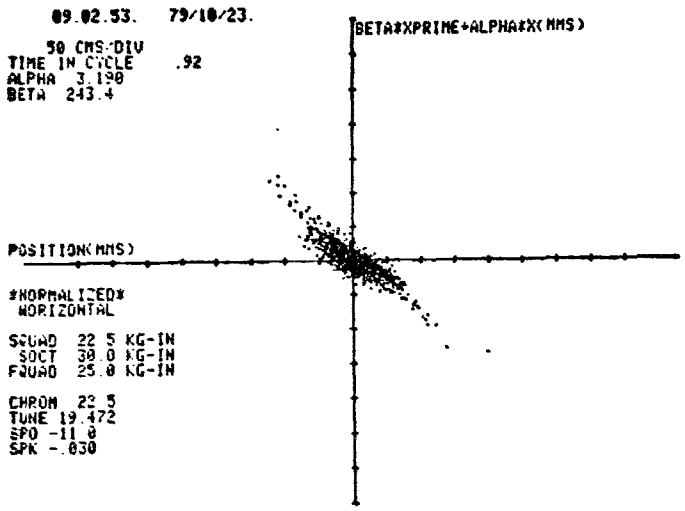
09.02.53. 79/10/23.
.50 CMS/DIV
TIME IN CYCLE .92
ALPHA 3.190
BETA 243.4
BETA*XPRIME+ALPHA*X(MMS)
POSITION(MMS)
NORMALIZED
HORIZONTAL
SQUAD 22.5 KG-IN
SOCT 30.0 KG-IN
FQUAD 25.0 KG-IN
CHROM 22.5
TUNE 19.472
SPO -11.0
SPK -.030

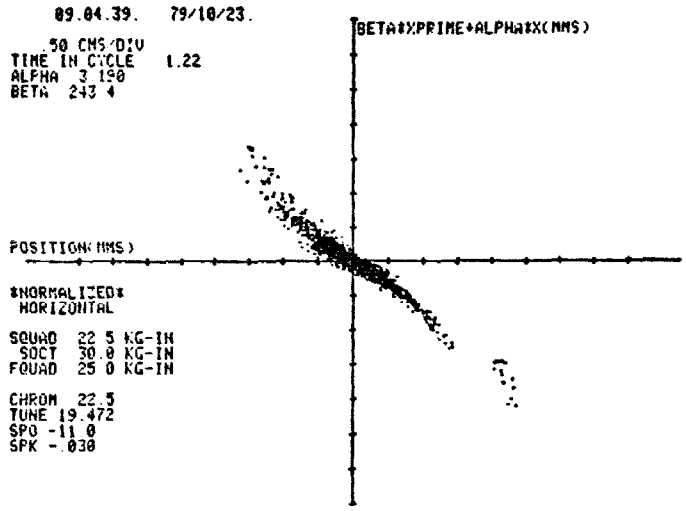
09.04.39. 79/10/23.
.50 CMS/DIV
TIME IN CYCLE 1.22
ALPHA 3.190
BETA 243.4
BETA*XPRIME+ALPHA*X(MMS)
POSITION(MMS)
NORMALIZED
HORIZONTAL
SQUAD 22.5 KG-IN
SOCT 30.0 KG-IN
FQUAD 25.0 KG-IN
CHROM 22.5
TUNE 19.472
SPO -11.0
SPK -.030

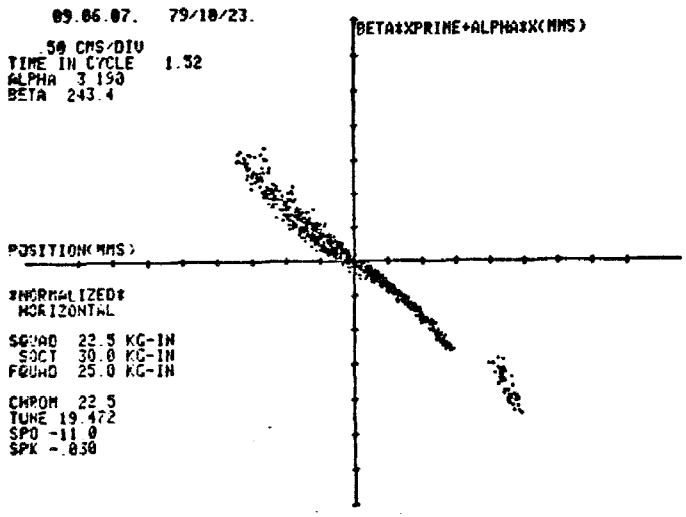
09.06.07. 79/10/23.
.50 CMS/DIV
TIME IN CYCLE 1.52
ALPHA 3.190
BETA 243.4
BETA*XPRIME+ALPHA*X(MMS)
POSITION(MMS)
NORMALIZED
HORIZONTAL
SQUAD 22.5 KG-IN
SOCT 30.0 KG-IN
FQUAD 25.0 KG-IN
CHROM 22.5
TUNE 19.472
SPO -11.0
SPK -.030

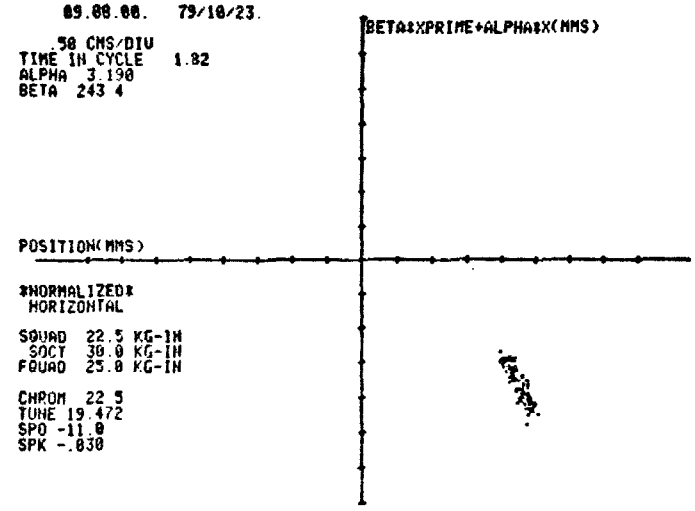
09.08.08. 79/10/23.
.50 CMS/DIV
TIME IN CYCLE 1.82
ALPHA 3.190
BETA 243.4
BETA*XPRIME+ALPHA*X(MMS)
POSITION(MMS)
NORMALIZED
HORIZONTAL
SQUAD 22.5 KG-IN
SOCT 30.0 KG-IN
FQUAD 25.0 KG-IN
CHROM 22.5
TUNE 19.472
SPO -11.0
SPK -.030

Fig. 13

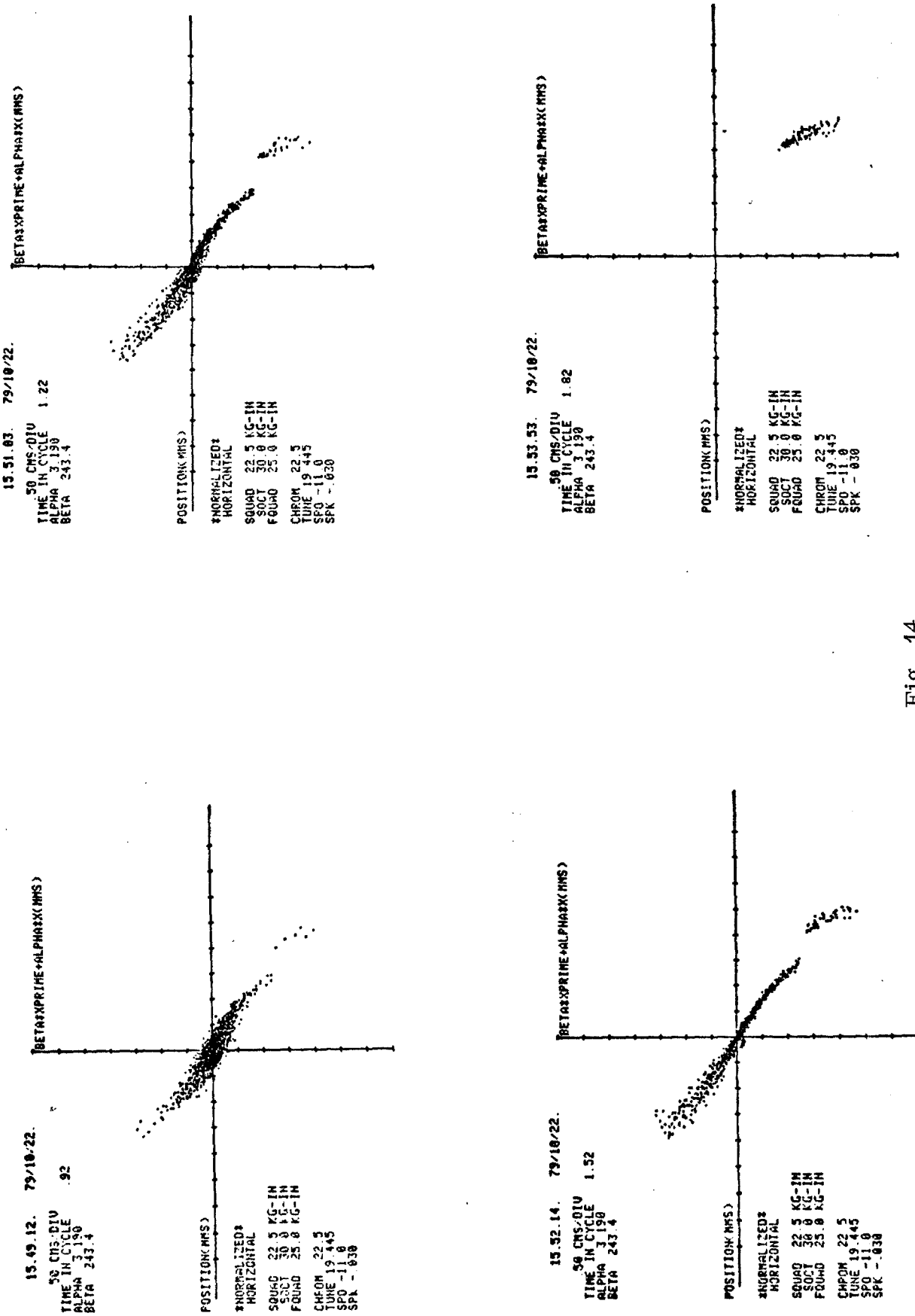
15.51.03. 79/10/22.
50 CMS/DIV 1.22
TIME IN CYCLE 3.190
ALPHA 243.4
BETA
BETA*XPRIME+ALPHA*X(MMS)
POSITION(MMS)
NORMALIZED
HORIZONTAL
SQUAD 22.5 KG-IN
SOCT 30.0 KG-IN
FQUAD 25.0 KG-IN
CHROM 22.5
TUNE 19.445
SPO -11.0
SPK -.030
15.53.53. 79/10/22.
50 CMS/DIV 1.82
TIME IN CYCLE 3.190
ALPHA 243.4
BETA
BETA*XPRIME+ALPHA*X(MMS)
POSITION(MMS)
NORMALIZED
HORIZONTAL
SQUAD 22.5 KG-IN
SOCT 30.0 KG-IN
FQUAD 25.0 KG-IN
CHROM 22.5
TUNE 19.445
SPO -11.0
SPK -.030
15.49.12. 79/10/22.
50 CMS/DIV .92
TIME IN CYCLE 3.190
ALPHA 243.4
BETA
BETA*XPRIME+ALPHA*X(MMS)
POSITION(MMS)
NORMALIZED
HORIZONTAL
SQUAD 22.5 KG-IN
SOCT 30.0 KG-IN
FQUAD 25.0 KG-IN
CHROM 22.5
TUNE 19.445
SPO -11.0
SPK -.030
15.52.14. 79/10/22.
50 CMS/DIV 1.52
TIME IN CYCLE 3.190
ALPHA 243.4
BETA
BETA*XPRIME+ALPHA*X(MMS)
POSITION(MMS)
NORMALIZED
HORIZONTAL
SQUAD 22.5 KG-IN
SOCT 30.0 KG-IN
FQUAD 25.0 KG-IN
CHROM 22.5
TUNE 19.445
SPO -11.0
SPK -.030

Fig. 14

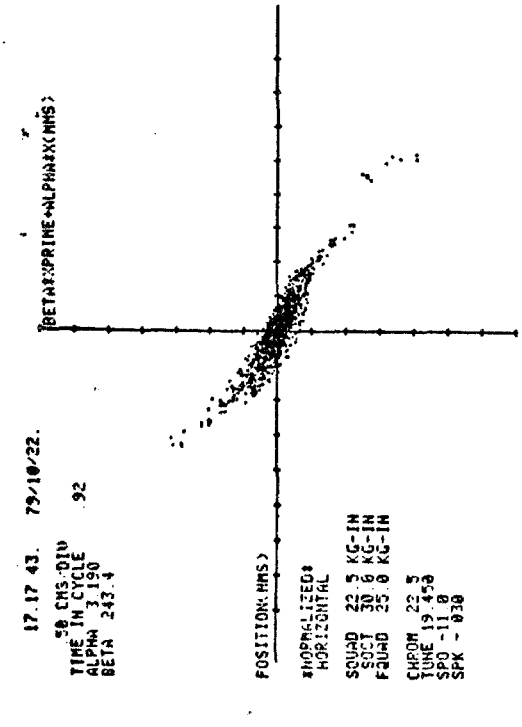
17.17.43. 79/10/22.
50 CMS/DIV
TIME IN CYCLE .92
ALPHA 3.190
BETA 243.4
BETA*XPRIME+ALPHA*XX(MMS)
POSITION(MMS)
NORMALIZED
HORIZONTAL
SQUAD 22.5 KG-IN
SOCT 30.0 KG-IN
FQUAD 25.0 KG-IN
CHROM 22.5
TUNE 19.450
SPO -11.0
SPK -.030

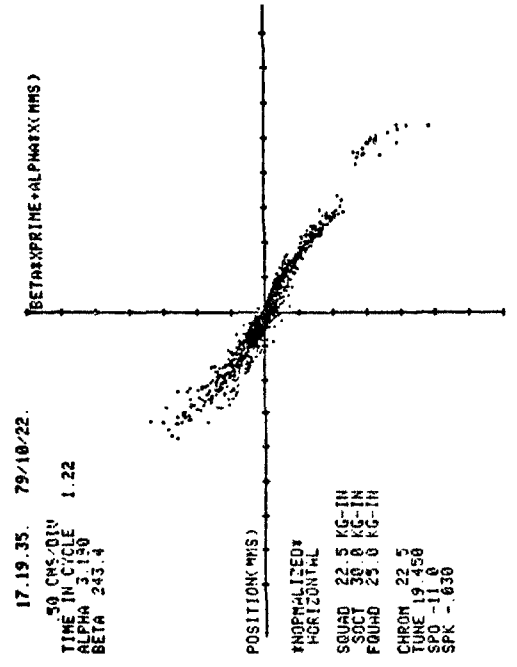
17.19.35. 79/10/22.
50 CMS/DIV
TIME IN CYCLE 1.22
ALPHA 3.190
BETA 243.4
BETA*XPRIME+ALPHA*XX(MMS)
POSITION(MMS)
NORMALIZED
HORIZONTAL
SQUAD 22.5 KG-IN
SOCT 30.0 KG-IN
FQUAD 25.0 KG-IN
CHROM 22.5
TUNE 19.450
SPO -11.0
SPK -.030

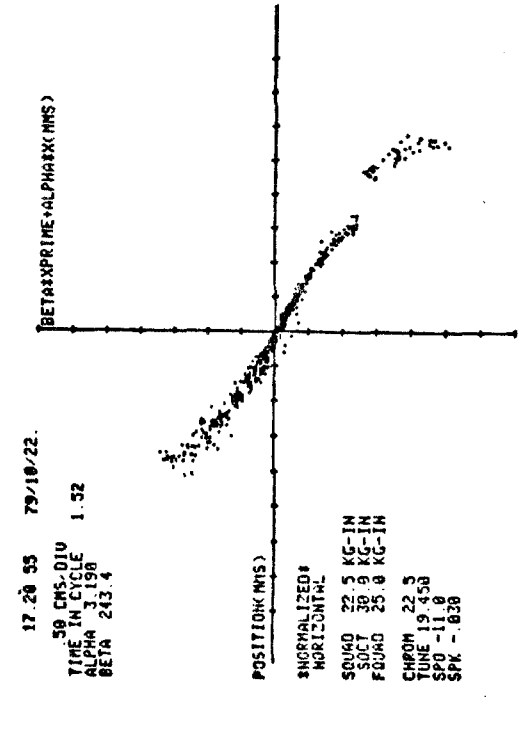
17.20.55 79/10/22.
50 CMS/DIV
TIME IN CYCLE 1.52
ALPHA 3.190
BETA 243.4
BETA*XPRIME+ALPHA*XX(MMS)
POSITION(MMS)
NORMALIZED
HORIZONTAL
SQUAD 22.5 KG-IN
SOCT 30.0 KG-IN
FQUAD 25.0 KG-IN
CHROM 22.5
TUNE 19.450
SPO -11.0
SPK -.030

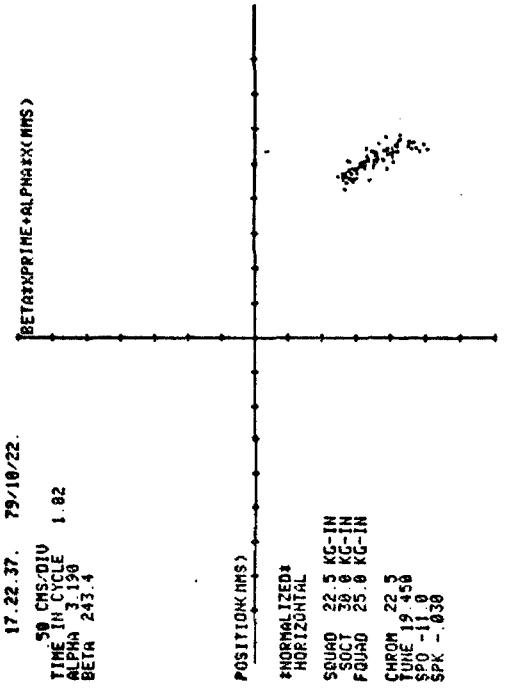
17.22.37. 79/10/22.
50 CMS/DIV
TIME IN CYCLE 1.82
ALPHA 3.190
BETA 243.4
BETA*XPRIME+ALPHA*XX(MMS)
POSITION(MMS)
NORMALIZED
HORIZONTAL
SQUAD 22.5 KG-IN
SOCT 30.0 KG-IN
FQUAD 25.0 KG-IN
CHROM 22.5
TUNE 19.450
SPO -11.0
SPK -.030

Fig. 15